W and Z Production in pp Collisions at 7 TeV with ATLAS

S. Prasad
Harvard University, Cambridge, MA 02138, USA

Measurements of W and Z cross-sections in pp collisions at $E_{\mathrm{CM}} = 7\,\mathrm{TeV}$ at the Large Hadron Collider are reported from the ATLAS experiment. From an observation of 118 leptonic W candidates, the inclusive W cross-section times leptonic branching fraction is measured as $[9.3 \pm 0.9(\mathrm{stat}) \pm 0.6(\mathrm{syst}) \pm 1.0(\mathrm{lumi})]\,\mathrm{nb}$. The result for the Z boson is $[0.83 \pm 0.07(\mathrm{stat}) \pm 0.06(\mathrm{syst}) \pm 0.09(\mathrm{lumi})]\,\mathrm{nb}$. These results agree with theoretical expectations from NNLO QCD.

I. INTRODUCTION, DATA SAMPLE AND OBJECT DEFINITIONS

Study of W and Z bosons at the turn-on of the Large Hadron Collider provides a high-statistics probe of the ATLAS [1] detector, in terms of characterizing tracking, lepton identification, lepton and missing energy scale and resolution, and trigger performance. Theoretically, measurements at the new energy of 7 TeV probe the proton at low-x, constraining parton density functions. The W and Z cross-sections are known at NNLO, giving a test of perturbative calculations. Also, these channels are important backgrounds for beyond SM processes. The data for these analyses come from the first LHC runs at 7 TeV, between March and July 2010. The datasets for the W and Z boson analyses are approximately $17\,\mathrm{nb}^{-1}$ and $225\,\mathrm{nb}^{-1}$ respectively, the luminosity being to known to 11%.

The analyses operate upon events from a collision bunch and both detector and machine status are used to select run periods for analysis. The data are compared to PYTHIA [2] samples processed with the ATLAS detector simulation software based on GEANT4 [3] and fully reconstructed. The trigger for the muon analysis uses hit patterns in dedicated chambers($|\eta| < 2.4$). The trigger efficiency is estimated at 88% (fully dominated by detector acceptance) using orthogonal jet-based triggers. The electron data are triggered in calorimetric towers that identify e/γ activity in a window of $|\eta| < 2.5$. A threshold of five trigger counts (5 GeV) is used. The efficiency of this trigger is better than 99.9%, with negligible uncertainty. Both e and μ analyses require a reconstructed vertex ($\geq$ three tracks) consistent with the beam spot. In addition, to reject cosmic rays and beam halo events, the muon analyses require that the primary vertex be found within 15 cm of the nominal position.

Electron measurements come from the energy of calorimeter clusters found in using a sliding-window approach. For electron identification, calorimetric shower shapes, hadronic leakage, track-cluster matching and impact parameter criteria are used. For the W analysis, purity is enhanced by requiring E/p compatibility between track and cluster, high-threshold transition radiation hits, and criteria to reject conversions. The analysis uses electrons with $p_T > 20\,\mathrm{GeV}$ in the region $|\eta| < 2.47$. The barrel-endcap transition region $|\eta| \in [1.37, 1.52)$ is excluded. Muon reconstruction combines tracking information in the Inner Detector (ID) the Muon Spectrometer (MS). Decays in flight are rejected with minimum p_{T} requirements on the MS track, and by imposing p_{T} compatibility between ID and MS track reconstructions. The cosmic ray contamination is reduced by requiring that the muon come from within 1 cm of a reconstructed vertex. Muons with $p_T > 20\,\mathrm{GeV}$ are used, with $|\eta| < 2.4$. To reduce QCD background, the summed p_{T} of tracks in a cone ($\Delta R = 0.4$) around the muon must be < 0.2 of muon p_{T}. Missing E_{T} is found using EM-scale calorimeter energy deposited in topological clusters, corrected for hadronic response, dead material and out-of-cluster losses. For muons, this is supplemented with the momentum, the muon's calorimeter deposition not being added to the calorimeter term. A requirement of 25 GeV is imposed for the W analysis.

II. EVENT SELECTION AND BACKGROUNDS

The W analysis requires that the transverse mass m_{T} of the candidate l - $E_{\mathrm{T}}^{\mathrm{Miss}}$ system, plotted in Fig. 1, be $m_{\mathrm{T}} \geq 40\,\mathrm{GeV}$. There are 46 (72) W $\to e\nu$ ($\mu\nu$) candidates. Electroweak (EW) backgrounds for W are obtained from

Monte Carlo predictions. In the electron channel, the EW background is $1.5 \pm 0.0\,(\mathrm{stat}) \pm 0.1\,(\mathrm{syst})$, coming chiefly from leptonic $\mathrm{W} \rightarrow \tau\nu$. The muon channel background of $4.4 \pm 0.0\,(\mathrm{stat}) \pm 0.3\,(\mathrm{syst})$, is dominated by $\mathrm{W} \rightarrow \tau\nu$ and $\mathrm{Z} \rightarrow \mu\mu$. The QCD background in $\mathrm{W} \rightarrow e\nu$ comes from hadrons misidentification, as well as electrons from conversion and heavy quark decay. It is estimated with a binned likelihood fit to data of Monte Carlo templates of calorimetric isolation, at $1.1 \pm 0.2\,(\mathrm{stat}) \pm 0.4\,(\mathrm{syst})$ events. The muon channel QCD background, mainly from heavy quark decay, is estimated by extrapolating from control regions in the E_T^{Miss} vs. isolation plane, at $0.9 \pm 0.3\,(\mathrm{stat}) \pm 0.6\,(\mathrm{syst})$. Z boson candidates are formed using pairs of oppositely charged leptons, with the invariant mass of the lepton pair required to be between 66 GeV and 116 GeV. 46 (79) candidates are observed in the $\mathrm{Z} \rightarrow e^+e^-$ ($\mu^+\mu^-$) channel, whose peak is shown in Fig. 2. The background for $Z \rightarrow e^+e^-$ is $0.49 \pm 0.07\,(\mathrm{stat}) \pm 0.05\,(\mathrm{syst})$. The background in the muon channel is $0.17 \pm 0.01\,(\mathrm{stat}) \pm 0.01 \pm (\mathrm{syst})$.

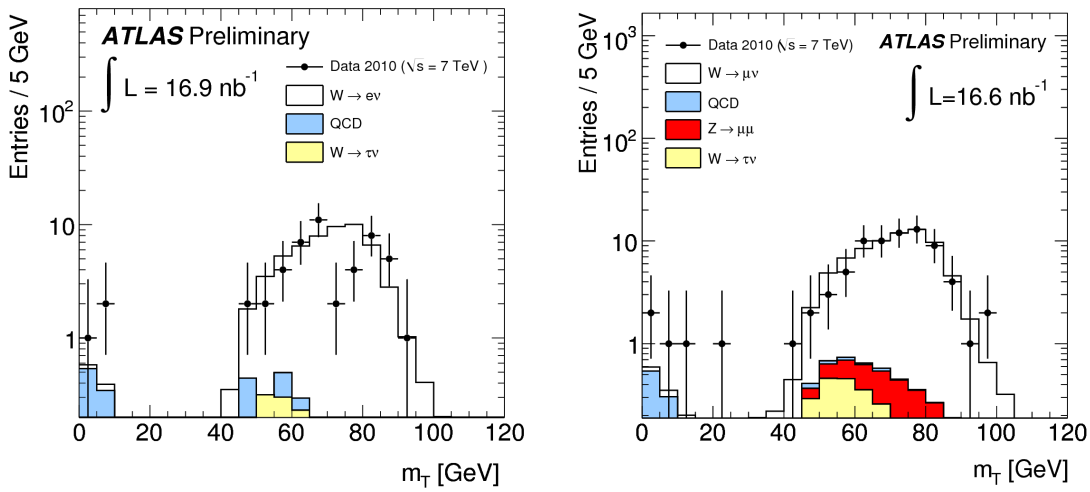

(a)$\mathrm{W} \rightarrow e\nu$ (b)$\mathrm{W} \rightarrow \mu\nu$

FIG. 1: Transverse mass m_{T} of the (a) $e - E_T^{\mathrm{Miss}}$ and (b) $\mu - E_T^{\mathrm{Miss}}$ systems, where $p_{\mathrm{T}}(l) > 20\,\mathrm{GeV}$ and $E_T^{\mathrm{Miss}} > 25\,\mathrm{GeV}$.

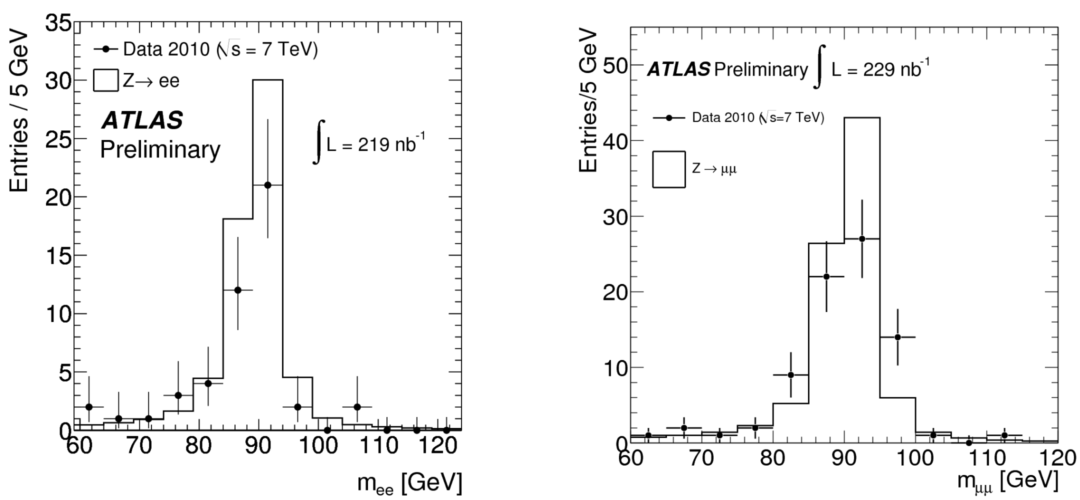

(a)$\mathrm{Z} \rightarrow e^+e^-$ (b)$\mathrm{Z} \rightarrow \mu^+\mu^-$

FIG. 2: Invariant mass m_{ll} of Z candidates for ee (a) and $\mu\mu$ (b). The background is suppressed because of its smallness.

III. CROSS-SECTION AND CONCLUSION

For N observed events and background estimate of N^{bkg} in a luminosity of L^{int}, we have:

$$\sigma_{\mathrm{W(Z)}} \times \mathrm{BR}_{\mathrm{W}\to l\nu(\mathrm{Z}\to ll)} = \frac{N - N^{\mathrm{bkg}}_{\mathrm{W(Z)}}}{A_{\mathrm{W(Z)}} C_{\mathrm{W(Z)}} L^{\mathrm{int}}_{\mathrm{W(Z)}}} \tag{1}$$

Here, A is the geometrical acceptance at generator level, while C is the ratio between the number of selected reconstructed events and the number of generated events in the fiducial region. The systematics on A_{W} and A_{Z} are estimated at 3%, from using different PDF sets and comparing MC@NLO and PYTHIA values. The uncertainty on C in the electron channel is 8% and 14% for W and Z, driven by the lepton identification. The muon systematic comes from the trigger, muon reconstruction and resolution, and from missing energy for the W. It is 7% in both the W and Z analyses.

The cross-section times leptonic branching fraction for W is $[8.5 \pm 1.3\,(\mathrm{stat}) \pm 0.7\,(\mathrm{syst}) \pm 0.9\,(\mathrm{lumi})]$ nb in the electronic channel and $[10.3 \pm 1.3\,(\mathrm{stat}) \pm 0.8\,(\mathrm{syst}) \pm 1.1\,(\mathrm{lumi})]$ nb for the muonic channel. The combined value is $[9.3 \pm 0.9\,(\mathrm{stat}) \pm 0.6\,(\mathrm{syst}) \pm 1.0\,(\mathrm{lumi})]$ nb. The Z $\to e^+e^-$ and Z $\to \mu^+\mu^-$ results are respectively $[0.72 \pm 0.11\,(\mathrm{stat}) \pm 0.10\,(\mathrm{syst}) \pm 0.08\,(\mathrm{lumi})]$ nb and $[0.89 \pm 0.10\,(\mathrm{stat}) \pm 0.07\,(\mathrm{syst}) \pm 0.10\,(\mathrm{lumi})]$ nb, for a combined result of $[0.83 \pm 0.07\,(\mathrm{stat}) \pm 0.06\,(\mathrm{syst}) \pm 0.09\,(\mathrm{lumi})]$ nb. These results are placed in historical context in Fig. 3, and in agreement with theoretical expectations of $\sigma_{W\to l\nu} = 10.46\,\mathrm{nb}$, and $\sigma_{Z/\gamma^*\to ll} = 0.99\,\mathrm{nb}$, computed at NNLO with 4% uncertainty using FEWZ [6] and MSTW2008 [7].

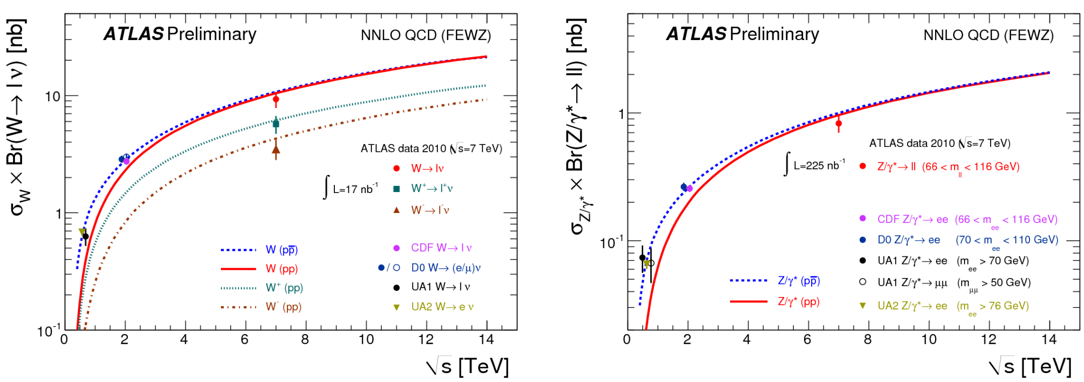

(a) $\mathrm{W} \to l\nu$ (b) $\mathrm{Z} \to l^+l^-$

FIG. 3: The measured values $\sigma_{\mathrm{W}} \times \mathrm{BRW} \to l\nu$ (a) and $\sigma_{\mathrm{Z}} \times \mathrm{BRZ}/\gamma^* \to l^+l^-$ (b), compared to NNLO QCD calculations and to previous measurements. The predictions are shown for both pp and $p\bar{p}$ colliders as a function of $\sqrt{s}$.

[1] ATLAS Collaboration, "The ATLAS Experiment at the CERN Large Hadron Collider", JINST 3 (2008) 003.

[2] T. Sjostrand, S. Mrenna, and P. Skands, "PYTHIA 6.4 physics and manual", JHEP 05 (2006) 026.

[3] GEANT4 Collaboration, S. Agostinelli et al., "GEANT4: A simulation toolkit", Nucl. Instrum. Meth. A506 (2003) 250.

[4] ATLAS Collaboration, "Measurement of the W $\to l\nu$ production cross-section and observation of Z $\to ll$ production in proton-proton collisions at $\sqrt{s} = 7\,\mathrm{TeV}$ with the ATLAS detector", ATLAS-CONF-2010-051.

[5] ATLAS Collaboration, "Measurement of the Z $\to ll$ production cross-section in proton-proton collisions at $\sqrt{s} = 7\,\mathrm{TeV}$ with the ATLAS detector", ATLAS-CONF-2010-076.

[6] C. Anastasiou, L. Dixon, K. Melnikov, and F. Petriello, "High-precision QCD at hadron colliders: electroweak gauge boson rapidity distributions at NNLO", Phys. Rev. D69 (2004) 094008.

[7] A. D. Martin, W. J. Stirling, R. S. Thorne, and G. Watt, "Parton distributions for the LHC", Eur. Phys. J. C63 (2009) 189-285.